

UCLA

UCLA Previously Published Works

Title

Asymmetric Beam Driven Plasma Wakefields at the AWA

Permalink

<https://escholarship.org/uc/item/4124s6f1>

Authors

Manwani, P
Ancelin, H
Yadav, M
et al.

Publication Date

2021

DOI

10.18429/JACoW-IPAC2021-TUPAB147

ASYMMETRIC BEAM DRIVEN PLASMA WAKEFIELDS AT THE AWA

P. Manwani*, H. Ancelin, M. Yadav¹, G. Andonian, J. Rosenzweig, UCLA, Los Angeles, CA, USA
G. Ha, J. Power, Argonne National Lab, Lemont, IL, USA
¹also at University of Liverpool, Liverpool, UK

Abstract

In future plasma wakefield acceleration-based scenarios for linear colliders, beams with highly asymmetric emittance are expected. In this case, the blowout region is no longer axisymmetric, but elliptical in cross-section, which implies that the focusing is not equal in the two transverse planes. In this paper, we analyze simulations for studying the asymmetries in flat-beam driven plasma acceleration using the round-to-flat-beam transformer at the Argonne Wakefield Accelerator. Beams with high charge and emittance ratios, in excess of 100:1, are routinely available at the AWA. We use particle-in-cell codes to compare various scenarios including a weak blowout, where the plasma focusing effect exhibits higher order mode asymmetry. Further, practical considerations for tunable plasma density using capillary discharge and laser ionization are compared for implementation into experimental designs.

INTRODUCTION

Beam based plasma wakefield accelerators (PWFA) operate in two main regimes - linear and nonlinear, or blowout, regime [1]. In the blowout case, the strong electric fields of the beam force the plasma electrons outward, resulting in a plasma column that is completely devoid of electrons. The collective separation of the plasma species leads to a wakefield that is essentially electrostatic in nature with the associated electric fields in the transverse and longitudinal directions. The scenario for the case of the axisymmetric beam has been studied extensively [2,3]. However, investigations into the asymmetric beam scenario are not as extensive in the literature, leaving a lot of scope to answer questions about the physics associated with plasma structures formed by asymmetric beams.

Asymmetric, or flat, beams have been studied in dielectric structures with slab geometries [4,5]. In order to mitigate radiation effects at the interaction point in a future collider application, one could use transversely asymmetric beams with asymmetric transverse emittances, also in PWFA scenarios. These beams could be produced using several approaches via round-to-flat transformations of beams having asymmetric emittances generated using a magnetized photocathode [6,7], and be used to analyze plasma dynamics that are not seen present in near-axisymmetric bunches.

SETUP OF EXPERIMENT

The AWA facility is an ideal location to test key concepts of the flat beam PWFA scenario, due to their recent experience in generating and characterizing asymmetric beams [7],

* pkmanwani@gmail.com

Table 1: Parameters for AWA

Parameter	Value	Unit
Beam		
Peak density, n_b/n_0	6.54	-
Energy, E_b	50	MeV
σ_z	674	μm
σ_x, σ_y	113, 11.3	μm
$\epsilon_{n,x}, \epsilon_{n,y}$	200, 2	$\mu\text{m} - \text{rad}$
Plasma		
Species	H ⁺	-
Density, n_0	1.4×10^{14}	cm^{-3}
Particles per cell	4	-
Simulation		
Simulation window (x,y,z)	(8, 8, 14)	k_p^{-1}
Grid	(1024) ³	-
Timestep	0.25	ω_p^{-1}
Beam particles	1.68×10^7	-

and recent experiments on PWFA interactions with shaped bunches [8]. Diagnostics at the AWA facility include a complete longitudinal characterization of the beam, before and after interaction with the plasma, using a deflector cavity and dipole spectrometer. Practical considerations for tunable plasma density generation include the use of high-voltage capillary discharge [9], and ionization of a plasma column in a dielectric capillary with a high intensity laser [10]. For the relatively modest plasma densities targeted by this experiment (see Table 1), the capillary discharge approach is adequate. Beam alignment through the plasma capillary is accomplished with two profile monitors immediately downstream and upstream of the capillary, which also yields valuable information on the beam focus and beam sizes during the interaction. The incorporation of multiple turbomolecular pumps near the plasma chamber, and the use of a rapid-action valve for gas introduction into the capillary to reduce gas load on the system, will allow for windowless operation [11]. This latter point is important, as any intercepting media (such as a window to prevent escape of gas in the beamline) would have an emittance spoiling effect for the asymmetric beam.

SIMULATION RESULTS

The simulations were performed using QuickPIC [12], a 3D quasi-static particle-in-cell code, to explore the general characteristics of the scheme. The simulations were first run with an axisymmetric beam to establish the regime of operation. The simulation parameters were kept the same as

those given in Table 1 but the emittance and beam spot sizes were kept equal in both transverse planes. The normalized transverse emittance, ϵ_{\perp} , is equal to $20 \mu\text{m} - \text{rad}$ and beam spot size, σ_{\perp} , is equal to $35.9 \mu\text{m}$. The plasma wake is concomitantly axisymmetric and both the beam and the weak blowout that is formed are shown in Fig. 1.

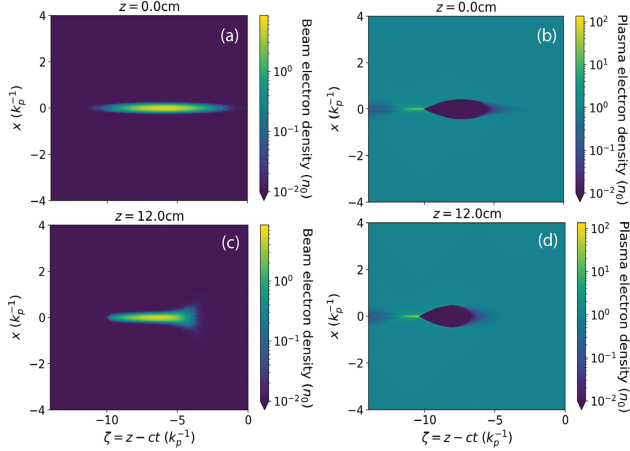


Figure 1: Beam and plasma electron densities for the symmetric AWA case at the initial time step (a-b) and after propagating a distance of 12cm (c-d).

These are followed by the simulations of the asymmetric beam using the parameters described in Table 1. The plasma wake is elliptical as can be seen in Fig. 2. The transverse forces in this elliptical blowout structure can be calculated analytically by approximating it as an infinitely long cylinder of ions with an elliptical cross section [13] and is given by:

$$E_x = \frac{en_0bx}{\epsilon_0(a+b)} = \frac{en_0x}{\epsilon_0(1+m)} \quad (1)$$

$$E_y = \frac{en_0ay}{\epsilon_0(a+b)} = \frac{en_0my}{\epsilon_0(1+m)}, \quad (2)$$

where a and b are the semi-major and semi-minor axis of the elliptical column respectively and $m = a/b$. In the transverse plane, where the beam is small, the beam is completely submerged in the ion cavity and strongly focused by the linear focusing forces which are linear and stronger in this dimension. In the other plane, the beam is larger than the ion column due to the weak blowout, causing head erosion of the beam electrons outside of the blowout region. The part of the beam inside the ion column is still linearly focused but the scaling factor of the focusing force is smaller. The transverse forces per unit charge, $\vec{F}/|q|$, along these planes are shown in Fig. 3. The single density spike that is observed in the axisymmetric case is replaced with a line of high density behind the blowout region. The evolution of the beam transverse emittances and spot sizes for this case are shown in Fig. 4.

EXTENSION TO FACET-II

We extend the flat beam case for possible application at the FACET-II facility [14] (see Table 2 for simulation

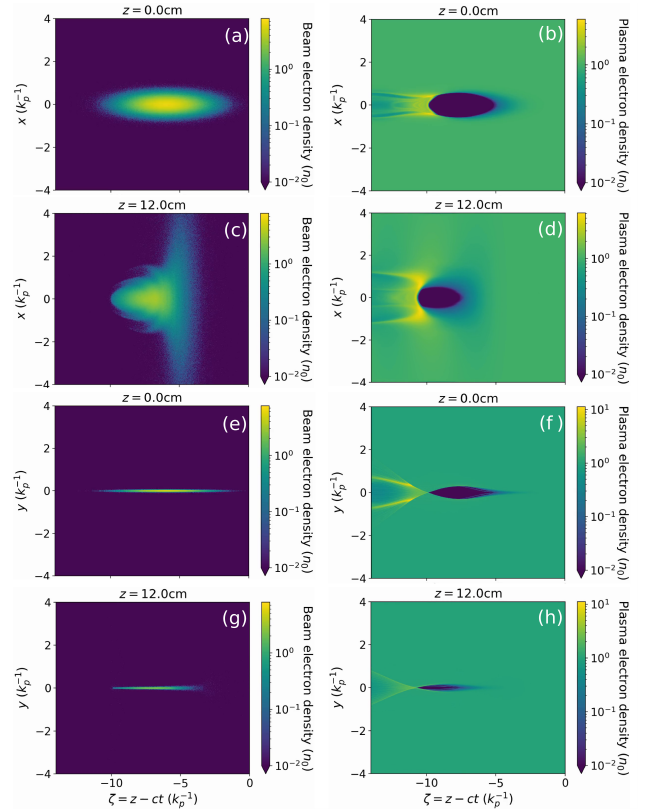


Figure 2: Beam and plasma electron densities for the asymmetric AWA case at the initial time step, x- ζ (a-b) y- ζ (e-f) and after propagating a distance of 12cm, x- ζ (c-d) y- ζ (g-h).

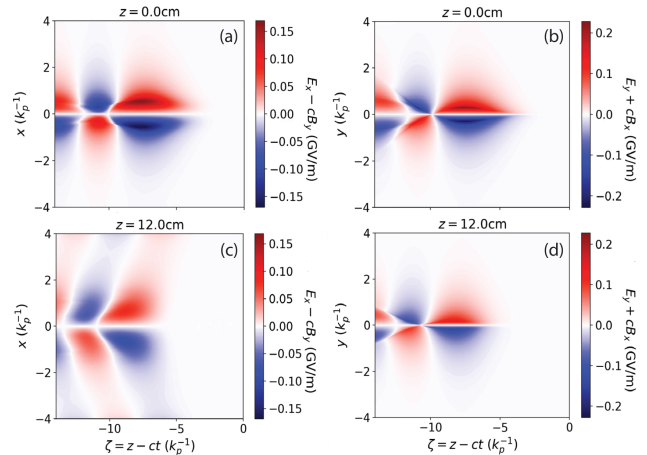


Figure 3: Transverse forces per unit charge, $\vec{F}/|q|$, for the asymmetric AWA case at the initial time step, x- ζ (a) y- ζ (b) and after propagating a distance of 12cm, x- ζ (c) y- ζ (d).

parameters), and explore the case where the beam density is much larger than the plasma density, $n_b \gg n_0$. The beam and strong blowout wake in this case are shown in Fig. 5 and it is significantly different from the AWA case as the wake is quite axisymmetric. The plasma wake initially overlaps with the beam but gradually increases in size to a maximum point in both the transverse planes. The beam is smaller than the blowout cavity in both transverse planes, and the

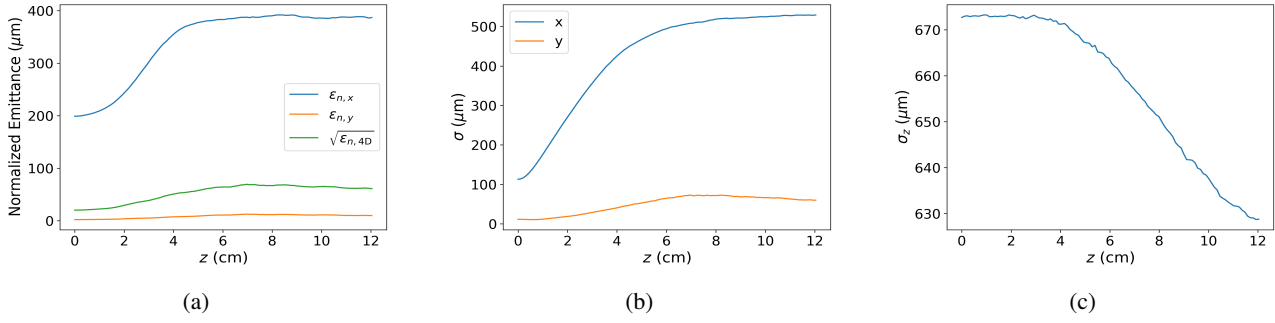


Figure 4: Evolution of the beam transverse emittances (a), spot sizes (b), and bunch length (c) for the asymmetric AWA case.

Table 2: Parameters for FACET

Parameter	Value	Unit
Beam		
Peak density, n_b/n_0	186	-
Energy, E_b	10	GeV
σ_z	20	μm
σ_x, σ_y	3.7, 0.37	μm
$\epsilon_{n,x}, \epsilon_{n,y}$	100, 1	$\mu\text{m} - \text{rad}$
Plasma		
Species	H^+	-
Density, n_0	1.5×10^{17}	cm^{-3}
Particles per cell	4	-
Simulation		
Simulation window (x,y,z)	(10, 10, 11)	k_p^{-1}
Grid	$(2048)^2 \times 1024$	-
Timestep	2.5	ω_p^{-1}
Beam particles	3.36×10^7	-

head erosion is notably reduced. The fields calculated earlier approach, $E_x = E_y = \frac{en_0 r}{2\epsilon_0}$, where r is the radial coordinate. This implies that the magnitude of the transverse forces no longer depends on the asymmetry of the beam, resulting in equal focusing in both the transverse planes. However, due to the intense beam density, there is significant asymmetric ion motion which would have nonlinear asymmetric effects.

Increasing the duration of the simulation in the cases described above resulted in the bifurcation of the beam, in which the beam splits into two equal halves. However, this bifurcation was dependent on the simulation parameters and is preliminarily attributed to a numerical instability. The source of the bifurcation is under current investigation, and may be a potential violation of the quasi-static assumption used in the simulation.

CONCLUSION

In this paper we have discussed the physics associated with elliptical wakes with weak blowout driven by asymmetric beams having high transverse emittance ratios. Understanding the plasma wakefield structure corresponding to these

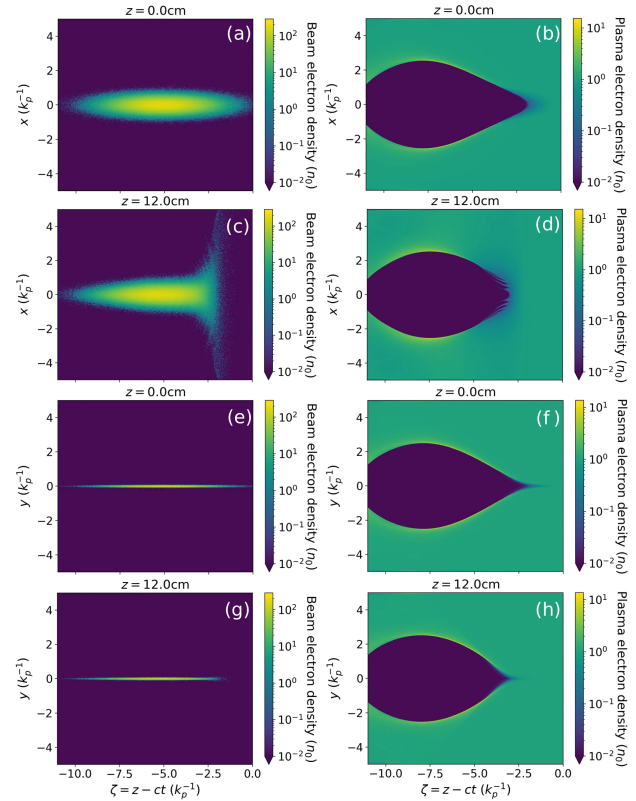


Figure 5: Beam and plasma electron densities for the asymmetric FACET case at the initial timestep, x- ζ (a-b) y- ζ (e-f) and after propagating a distance of 12cm, x- ζ (c-d) y- ζ (g-h).

flat beams is important as these beams are demanded for future linear collider scenarios to mitigate beamstrahlung at the interaction point [15].

ACKNOWLEDGEMENTS

This work was performed with the support of the US Department of Energy, Division of High Energy Physics under Contract No. DE-SC0017648 and DE-SC0009914. This work used computational and storage services associated with the SCARF cluster provided by the STFC Scientific Computing Department.

REFERENCES

- [1] N. Barov, J. B. Rosenzweig, M. E. Conde, W. Gai, and J. G. Power, "Observation of plasma wakefield acceleration in the underdense regime", *Phys. Rev. ST Accel. Beams*, vol. 3, p. 011301, Jan. 2000. doi:10.1103/physrevstab.3.011301
- [2] J. B. Rosenzweig, B. Breizman, T. Katsouleas, and J. J. Su, "Acceleration and focusing of electrons in two-dimensional nonlinear plasmawake fields", *Phys. Rev. A*, vol. 44, pp. R6189–R6192, Nov. 1991. doi:10.1103/physreva.44.r6189
- [3] W. Lu, C. Huang, M. Zhou, W. B. Mori, and T. Katsouleas, "Nonlinear theory for relativistic plasma wakefields in the blowout regime", *Phys. Rev. Lett.*, vol. 96, p. 165002, Apr. 2006. doi:10.1103/PhysRevLett.96.165002
- [4] B. D. O'Shea *et al.*, "Suppression of deflecting forces in planar-symmetric dielectric wakefield accelerating structures with elliptical bunches", *Phys. Rev. Lett.*, vol. 124, p. 104801, Mar. 2020. doi:10.1103/PhysRevLett.124.104801
- [5] S. S. Baturin, G. Andonian, and J. B. Rosenzweig, "Analytical treatment of the wakefields driven by transversely shaped beams in a planar slow-wave structure", *Phys. Rev. Accel. Beams*, vol. 21, p. 121302, Dec. 2018. doi:10.1103/PhysRevAccelBeams.21.121302
- [6] Tianzhe Xu *et al.*, "Generation High-Charge of Flat Beams at the Argonne Wakefield Accelerator", in *Proc. 10th International Particle Accelerator Conference (IPAC'19)*, Melbourne, Australia, May 2019, pp. 3337-3340. doi:10.18429/JACoW-IPAC2019-WEPTS094
- [7] A. Halavanau, J. Hyun, D. Mihalcea, P. Piot, T. Sen, and C. Thangaraj, "Magnetized and Flat Beam Experiment at FAST", in *Proc. 8th International Particle Accelerator Conference (IPAC'17)*, Copenhagen, Denmark, May 2017, pp. 3876-3879. doi:10.18429/JACoW-IPAC2017-THPAB073
- [8] R. Roussel *et al.*, "Single Shot Characterization of High Transformer Ratio Wakefields in Nonlinear Plasma Acceleration", *Phys. Rev. Lett.*, vol. 124, no. 4, p. 044802, Jan. 2020. doi:10.1103/physrevlett.124.044802
- [9] S. Barber, "Plasma Wakefield Experiments in the Quasi Non-linear Regime", Ph.D. thesis, University of California, Los Angeles, CA, USA, 2014.
- [10] N. Norvell *et al.*, "Gas sheet ionization diagnostic for high intensity electron beams", presented at the 12th Int. Particle Accelerator Conf. (IPAC'21), Campinas, Brazil, May 2021, paper MOPAB140.
- [11] G. Andonian *et al.*, "Status on a laser injection in beam driven dielectric wakefield accelerator experiment", *10th Int. Particle Accelerator Conf. (IPAC'19)*, Melbourne, Australia, May 2019, p. 3761. doi:10.18429/JACoW-IPAC2019-THPGW073
- [12] C. Huang *et al.*, "Quickpic: A highly efficient particle-in-cell code for modeling wakefield acceleration in plasmas", *J. Comp. Phys.*, vol. 217, no. 2, pp. 658 – 679, 2006. doi:10.1016/j.jcp.2006.01.039
- [13] M. R. Shubaly, "Space charge fields of elliptically symmetrical beams", *Nucl. Instrum. Methods*, vol. 130, no. 1, pp. 19–21, 1975. doi:10.1016/0029-554X(75)90150-0
- [14] V. Yakimenko *et al.*, "FacetII facility for advanced accelerator experimental tests", *Phys. Rev. Accel. Beams*, vol. 22, p. 101301, Oct. 2019. doi:10.1103/PhysRevAccelBeams.22.101301
- [15] Pisin Chen, "Differential luminosity under multiphoton beamstrahlung", *Phys. Rev. D*, vol. 46, pp. 1186–1191, Aug. 1992. doi:10.1103/PhysRevD.46.1186